γ

CONF-8706113--5

UCRL- 97262
PREPRINT

SEP 0 9 1987

HEAVY ION PRECOMPOUND PHENOMENA: A GLANCE AT HARD GAMMA & SUBTHRESHOLD PION PRODUCTION

MARSHALL BLAND
BRUCE A. REMINGTON

THIS PAPER WAS PREPARED FOR SUBMITTAL TO
VIth ADRIATIC CONFERENCE ON
FRONTIERS OF HEAVY ION PHYSICS
DUBROVNIK, YUGOSLAVIA
JUNE 15-19, 1987

AUGUST 1987

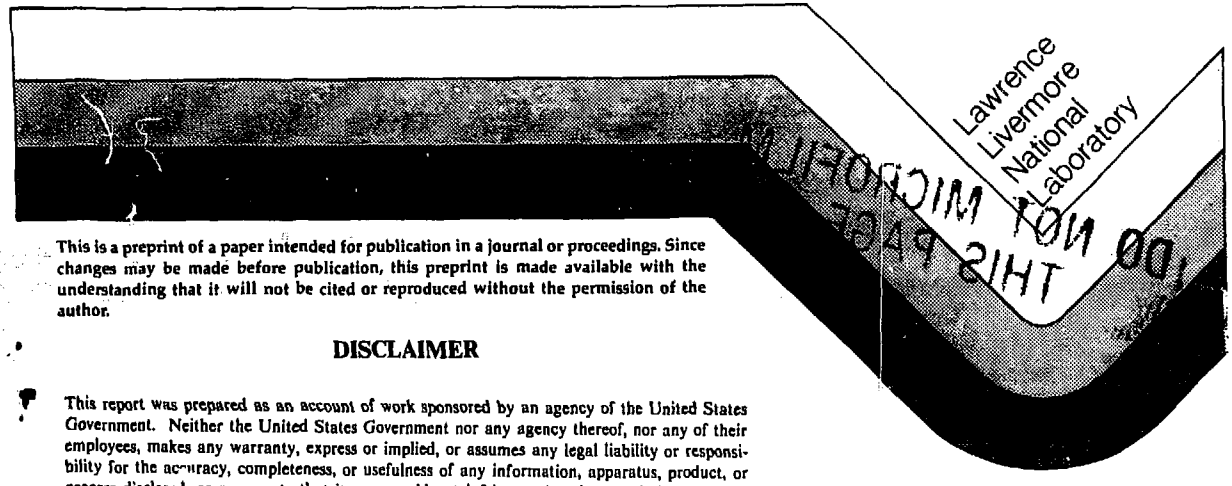

This is a preprint of a paper intended for publication in a journal or proceedings. Since changes may be made before publication, this preprint is made available with the understanding that it will not be cited or reproduced without the permission of the author.

DISCLAIMER

This report was prepared as an account of work sponsored by an agency of the United States Government. Neither the United States Government nor any agency thereof, nor any of their employees, makes any warranty, express or implied, or assumes any legal liability or responsibility for the accuracy, completeness, or usefulness of any information, apparatus, product, or process disclosed, or represents that its use would not infringe privately owned rights. Reference herein to any specific commercial product, process, or service by trade name, trademark, manufacturer, or otherwise does not necessarily constitute or imply its endorsement, recommendation, or favoring by the United States Government or any agency thereof. The views and opinions of authors expressed herein do not necessarily state or reflect those of the United States Government or any agency thereof.

DISTRIBUTION OF THIS DOCUMENT IS UNLIMITED

Heavy Ion Precompound Phenomena: A Glance at Hard Gamma and Subthreshold Pion Production *

Marshall Blann and Bruce A. Remington

UCRL--97262

DE87 014353

Abstract

We test a relaxation model based on two body nucleon-nucleon scattering processes to interpret phenomena observed in heavy ion reactions. We use the Boltzmann master equation to accomplish this. By assuming that the projectile nucleons share the total excitation with equal a-priori probability of all configurations, we are able to reproduce several sets of neutron spectra from ^{20}Ne and ^{12}C induced reactions on ^{165}Ho. With no additional free parameters our model successfully reproduces subthreshold pion production cross sections, high energy γ-ray spectra, and angular distributions of high energy γ-rays.

I. Introduction

As heavy ion reaction studies progressed from beam energies below 10 MeV/nucleon into the medium energy range, many non-equilibrium reaction phenomena have been observed. Nucleons are emitted with velocities far in excess of the beam velocity and with cross sections orders of magnitude above the equilibrium expectation.[1-3] Pions have been observed at incident energies per nucleon much less than the free nucleon-nucleon threshold energy.[4-7] Gamma-rays in excess of 100 MeV have been observed at incident energies as low as 20 to 30 MeV per nucleon.[8-13]

The intriguing question is how so much of the total energy available in the reaction entrance channel becomes focused on a single entity in the exit channel. We try to understand and interpret these phenomena in terms of nuclear models or nuclear theories.

One fascinating and quite successful approach is due to Greiner and his colleagues,[15] and is based on a collective bremmstrahlung

MASTER

*This work was performed under the auspices of the U.S. Department of Energy by Lawrence Livermore National Laboratory under contract No. W-7405-Eng-48.

DISTRIBUTION OF THIS DOCUMENT IS UNLIMITED

resulting from the slowing down of target and projectile nuclei as the nuclear densities start to overlap. Many other approaches rely on a mechanism due to incoherent nucleon-nucleon scattering processes in the nuclear field.[16-24] In this presentation we would like to attempt an explanation of all these phenomena in a very physically transparent model of the latter type. The numerical approach we will take will be the Boltzmann Master Equation (BME), originally applied to nucleon induced reactions by Harp et al.[25,26]

I shall first describe the physical model we use and the mathematical method of computer solution. Next we will test the one parameter of the model which we guess (based on earlier precompound studies with alpha particles) by comparing with experimental (HI,n) spectra. We will investigate changes required to treat pion production by the introduction of experimental NNπ cross sections,[27] and see how well these results, with no parameter adjustment, agree with the available data.

Next we will consider the question of NNγ cross sections as a function of energy, and see how well the BME reproduces absolute nucleus-nucleus and nucleon-nucleus γ-ray spectra,[28] with no free parameters. Then we will investigate the γ-ray angular distributions predicted by this model, and compare them with the available data.[8-13] Finally we will present our conclusion as to whether or not the incoherent N-N collision mechanism is one of the viable explanations for these many non-equilibrium phenomena.

2. Physics and Formulation of the Boltzmann Master Equation

In Fig. 1 we see a diagrammatic representation of the reaction of two heavy ions. In the upper portion of the figure we see two nuclei approaching one another in a geometric representation. The nuclei each have a spherical shape, with the nucleons bound inside each nucleus by the surface tension. Once the two nuclei touch, the interface disappears, and the surface tension and beam momentum combine in the coalescence process.

In the lower portion of Fig. 1 we represent the same reaction in an energy space represented by the potential wells of the two nuclei. The formation of the neck described in the geometric picture means that the nucleons of target and projectile may now begin to interact in some joint potential well formed in the coalescence process, in a time dependent manner. This energy space is the representation used in the BME.

The mathematical approach used in solving this problem is partly defined in Fig. 2, where we clarify the indexing used in the potential of the coalesced nuclear system. The model is based on nucleon-nucleon (N-N) collisions using free NN scattering cross sections to define collision rates W_{ij}, where

$$\omega_{ij\to klm}^{pn\gamma} = \frac{\sigma_{\gamma pn}[(2/M)(\varepsilon_i^n+\varepsilon_j^p)]^{1/2}}{V\sum'_{nop} g_n g_o g_p} \tag{1}$$

with symbols defined in Table 1. Having defined the intranuclear scattering rates, we may express the set of master equations as

$$dN_i^\chi/dt = g_i^\chi \sum_\gamma \Big\{ \sum'_{jkl} [\omega_{kl\to ij}^{\chi\gamma} g_k^\chi g_l^\gamma g_j^\gamma n_k^\chi n_l^\gamma (1-n_i^\chi)(1-n_j^\gamma) - \omega_{ij\to kl}^{\chi\gamma} g_j^\gamma g_k^\chi g_l^\gamma n_i^\chi n_j^\gamma (1-n_k^\chi)(1-n_l^\gamma)] - n_i^\chi \omega_{i\to i'}^\chi \Big\} + f_i(p,n). \tag{2}$$

with an analogous expression for neutron population relaxation processes. The dfus/dt term is a source term, representing a time dependent injection of nucleons and excitation energy during the coalescence (fusion) process; this term will be discussed shortly. The $(1-n_i)$terms give the Pauli exclusion. A more thorough discussion of the BME, as encoded originally by Harp, Miller, and Berne, and later modified by Blann, may be found in refs. 16, 25, 26.

There is still the question of the rate and energy distribution of nucleons injected during coalescence in a heavy ion reaction, namely, the source term of Eq. 2. How to calculate and model this is a very interesting and still very open question. In the limit of a light projectile on a heavy target we might expect a random energy conserving distribution, where the projectile nucleons A_p share the

total energy; we may assume that the many possible couplings of beam velocity and Fermi velocity will cause a randomized sharing of this energy, e.g. that every partition occurs with equal a-priori probability. We will do this, and then test the assumption against as broad a range of appropriate heavy ion data as possible. This assumption worked well for light ion induced reactions such as (α,p),[29,30] and we will see if it has some merit for heavy ion reactions as well.

Cindro and his collaborators have made many fine contributions in this regard by finding the best 'exciton number' parameter to describe a wide range of heavy ion induced reactions.[31] This work is important for understanding the detailed dependence of the exciton energy distributions on e.g. angular momentum and impact parameter, and perhaps on injection energy. Scobel and co-workers are currently working on putting this physics directly into the BME.[32]

For the present I wish to take a less detailed look at our assumption and see if, within the experimental uncertainties, it allows us to globally reproduce nucleon spectra from reasonably central collisions. By implication, if we have a reasonable representation of the initial nucleon energy distribution, we may use the model to see if this distribtuion in turn causes the other phenomena via the N-N collision process.

The results of the calculation are not very sensitive to the assumed rate of injection. We assume injection based on the volume of the projectile passing through a plane with a velocity equal to the beam velocity (cm system) reduced appropriately for the Coulomb barrier. We next compare calculated and experimental (HI,n) spectra from several reactions to test the assumptions of our model.

3. Comparisons of Calculated and Experimental Results

3.1 (HI,n) Spectra

In Fig. 3, we show comparisons between evaporation residue (ER)

and fission fragment (FF) gated, angle integrated neutron spectra from the ^{20}Ne bombardment of ^{165}Ho,[2] and the ER gated neutrons from the ^{12}C + ^{165}Ho reactions.[3]. The "experimental results" are parameterized angle integrated points for the "fast" component. We show calculated results for these spectra using n=20 for ^{20}Ne induced reactions and n= 12 for the ^{12}C induced reactions. The value of $n = A_p$ seems to give a satisfactory fit to all the data within uncertainties due to the angle integration method used. I should emphasize that the absolute values of the calculated spectra are compared with the experimental results in Fig. 3 without any normalization, and are all calculated without adjustment of the nucleon-nucleon mean free path.

The BME may be seen to give a quite satisfactory agreement for an a-priori calculation over a broad range of incident energies and projectiles, yielding spectra correct in shape and magnitude, without normalization of the spectral intensities. We will use the assumption of $n = A_p$ for the remainder of this work, with the word of caution that we have only shown a justification for the systems shown in Fig. 3. We are therefore extrapolating in the absence of the desired experimental data when we treat other systems.

3.3 Subthreshold Pion Production

Early on, Bertsch[33] suggested that the Fermi momentum and relative nucleon motion might couple in heavy ion reactions to give nucleons sufficient energy to produce pions via a N-N collision mechanism. Arndt and VerWest have tabulated excitation functions for N+N → N+N + pion. We should be able to add these channels to the BME to probe the possibility of the N-N collision process as a viable subthreshold pion production mechanism.[18] The input nucleon spectra for these calculations have been calculated with all energy partitions equally likely, but with no nucleon having more than $(\sqrt{\epsilon_f} + \sqrt{\epsilon_{beam}})^2$ units of energy where ϵ_f is the projectile Fermi energy and ϵ_{beam} is the beam energy per nucleon. We assumed $n=A_p$ which,

recalling the recent Berlin results (Fig. 3), gave excellent agreement between calculated and measured nucleon spectra in the pion production energy range. The rate equations for pions may be represented by:[18]

(3)

with the collision rate expressions given by:[18]

(4)

We use the experimental NNπ^0 production rates due to Verwest and Arndt.[27] Results of these calculations via the BME for a fairly broad range of experimentally measured systems are summarized in Table 2. The calculated yields include a crude π^0 emission attenuation factor estimated for a 2 fm mean free path. More details may be found in Ref. 18. The results are also quite sensitive to the value of the Fermi energy assumed for the projectile, which was 35 MeV in all cases. We might, for example expect lower values for the lightest projectiles. In view of the uncertainties of these calculations, we subjectively feel that agreement within a factor of 3-4 between calculated and measured yields is confirmation that the N-N collision is one (but by no means the only) viable mechanism for subthreshold pion production. This is seen to be the case for all the systems summarized in Table 2, except $^{40}Ca + {}^{40}Ar$, where the discrepancy is a factor of five, and for the 25 MeV/nucleon data. For the latter, we reasonably reproduce the O+Ni data if we assume a target Fermi energy of 30 MeV. Even this fails for the O+Al case. This, however, does not exclude the N-N mechanism, it merely requires smaller collision angles than the 90° assumed in the present application of the BME. For alternative explanations one should e.g., read the interesting nucleus-nucleus bremsstrahlung model due to Greiner and his collaborators.[14]

3.4 Production of High Energy γ-Rays

3.41 Energy Distributions

The BME may be modified for γ-ray production by addition of the rate for inelastic NNγ scattering,[19]

$$\frac{d^2N}{dE_\gamma d\Omega_\gamma} = \frac{1}{E_\gamma}\frac{\alpha}{(2\pi)^2}\sum_{k=1}^{2}\left|\frac{\hat{\varepsilon}_k\cdot\beta_i}{1-\hat{q}\cdot\beta_i} - \frac{\hat{\varepsilon}_k\cdot\beta_f}{1-\hat{q}\cdot\beta_f}\right|^2 P_{fac}(1+X). \tag{5}$$

with symbols as defined in Table I. We need not consider nnγ or ppγ rates, because these quadrupole cross sections are expected to be much smaller than the pnγ dipole cross section.[34] This rate, given in Eq. 5, is entered into the BME (Eq. 2) and we sum over all np collisions to give the total rate of production of γ-rays of energy m

$$d^2N_m^\gamma/dE\,dt = \sum_{ijkl}{}' \omega_{ij}^{pn\gamma}{}_{klm} g_i^n g_j^p g_k^n g_l^p n_i^n n_j^p (1-n_k^n)(1-n_l^p). \tag{6}$$

We use a semi-classical radiation formula with two modifications, to calculate the γ-ray yield per np collision.[19,35,36]

(7)

In (7) $\alpha = 1/137$ is the fine structure constant, β_i and β_f are the initial and final proton velocities (in units of c) and $\hat{e}_1$, $\hat{e}_2$ and $\hat{q}$ are the unit vectors for the two directions of polarization and the γ-ray propagation direction. The modifications to the semi classical formula are given in the last two factors. Of these $P_{fac} = \beta_f\gamma_f/\beta_i\gamma_i$ is a final state phase space correction.[36]. The (1+X) factor allows the magnitude of (7) to be varied. It was suggested[34] that failure of eq. (7) to include meson exchange processes should require $X \gtrsim 1$ as a correction. This approximation may be tested against the p+d→ γ spectrum of Edgington and Rose,[28]

measured with 140 MeV protons (Fig. 4). Because $pp\gamma << pn\gamma$,[34] the deuteron target approximates a neutron target with some internal motion. In Fig. 4 we see the result of Eq. (7) with X=0, but averaged over the target neutron internal motion,[37] and the latter result with X=1. The agreement is quite satisfactory, so we use X = 1 for the remainder of this work.

Neuheuser and Koonin have recently evaluated the quantum mechanical analog of Eq.(7)[38]. We show their result in Fig. 4 also. Because the agreement with the $d(p,\gamma)$ spectrum is poor we do not adopt this result; we will, however, show results of this formulation in several figures. A weakness of our reliance on Eq. (7) with X=1 confirmed by the $d(p,\gamma)$results is that we have only the 140 MeV data set. Clearly similar data sets at other incident proton energies would be extremely valuable to confirm our reliance on Eq. (7) with X = 1.

We include results of a broader nucleus Fermi momentum and further test Eq. (7) by using it with Eqs. (5) and (6) in the BME for the $^{12}C(p,\gamma)$ and $Pb(p,\gamma)$ inclusive spectra[28] shown in Fig. 4. The agreement, with no normalization (having accepted X = 1 in Eq. (7)) is excellent. Next we perform the calculation for nucleus-nucleus data sets, using all published results we were aware of. These results are presented in Figs. 5-9.

In Fig. 5 we show the results of Stevenson et al.[8] who used a stack of lucite as Cerenkov detectors. The agreement of spectra calculated with no parameter variation, is excellent. The quantal result[38] gives spectra which are a little high. In Figs. 6 and 7 we see results of Nifenecker et al, using ^{40}Ar[9] and ^{86}Kr projectiles[10] at 30 and 44 MeV/u, respectively. This represents an extrapolation of the assumptions on nucleon distributions based on results shown in Fig. 3. Nonetheless we find excellent agreement between calculated and experimental results. These data were measured with a stack of plastic scintillators followed by a NaI detector. In fig. 8 we show results of Alamanos et al. for 35 MeV/u ^{14}N reactions on Ni nuclei[11] measured with lead glass detectors; our calculation fails to reproduce these data satisfactorily.

In fig. 9 we show the results of Grosse et al[12,13] for 48-84

MeV/μ ^{12}C projectiles on ^{12}C and ^{238}U targets. Again our calculation seriously underestimates the data. The quantal result, on the other hand, is in satisfactory agreement with these data. Lead glass detectors were used in measuring the data in Fig. 9.

We follow an idea from Morrissey[39] in Fig. 10 and integrate the experimental and calculated γ spectra for E_γ>50MeV, showing the results scaled by reaction cross section plotted versus the beam energy. At the lower energies, calculation and experiment are in quite reasonable agreement. At the higher energies there is a divergence. This may represent the appearance of a second mechanism at the higher energy (e.g. coherent nucleus-nucleus bremmstrahlung),[14] it may represent a difference in calibrations between lead glass and plastic scintillator /NaI detectors, or a breakdown of Eq. (7) for higher nucleon collision energies. This is an open question and an important question to answer as more data become available.

3.4 Gamma-Ray Angular Distributions

Since Eq. (7) has an angular dependence for the γ-ray, we may treat the (relativistic) kinematics for the nucleon-nucleon scattering process and calculate the γ-ray angular distribution. We first do this for the d(p,γ) case where we average over the neutron internal momentum. We compare this absolute calculation with the data of Edgington and Rose [28] in Fig. 11; the agreement is excellent. We also compare with data for the ^{12}C (p,γ) inclusive reaction (Fig. 11). The latter calculation is arbitrarily normalized in magnitude in order to compare the shape of the angular distribution, which is also in quite reasonable agreement with the experimental result.

We next consider heavy ion reactions. Here we must consider two additional complications over the d(p,γ) case. First, the coupling of the Fermi and beam velocities leads to an energy spread and an angular spread about the beam axis for the injected nucleons. Second, for lower energy γ-rays we must consider not only first collision

processes, but also higher order collisions. We use the BME to make this division. We then make the overestimate that higher order collisions give an isotropic γ-ray angular distribution, while the first collision contribution comes from Eq. (7) folded over initial injection angles and averaged over Fermi momenta.

Results of these relative calculations are shown in Fig. 12 for the data of Stevenson et al.[8] The calculated results are in quite reasonable agreement with the data which are between the first and multiple collision limits given. We have made a similar comparison for the data of Grosse et al[12,13] for which we get similarly good agreement,and of Alamanos et al, for which we do not. On the whole, the NNγ mechanism seems to give quite satisfactory agreement with the major share of experimental data for many γ-ray energies.

IV. Conclusions

The BME model is transparent in the physics used to treat the equilibration process, specifically, a series of N-N collisions determined by free scattering cross sections moderated by the Pauli exclusion principle. The BME is very versatile and it is easy to use to test ideas; e.g., pion production cross-sections, incomplete momentum transfer. The model works quite well in reproducing nucleon emission spectra for central collision processes using an input distribution based on $n = A_p$. More work needs to be done in modeling the initial distribution function with the coupling constraints, phase space constraints, and with consideration of angular momentum averaging.

A broader range (projectile and projectile energy variations) of nucleon and cluster emission spectra gated on central collisions would be welcome as a more severe test of the BME and other precompound decay models. Measurement of nucleons at the highest kinetic energies may give crucial information on the microscopic details of the coalescence process, in particular the coupling of relative motion and Fermi motion of the projectile nucleons, and of the viability of the N-N collision process for subthreshold pion production.

All caveats considered, simple precompound decay models yield a wealth of insight into the dynamics of heavy ion reactions. Many of the predictions, made as early as 1974 by use of these models [16,40] are now being realized in experimental measurements. These models should continue to be strong tools in the interpretation of heavy ion reactions. We have shown that all the phenomena analyzed in this work may be interpreted in terms of a N-N collision mechanism, getting excellent agreement with nearly all data without parameter variation. Similar tests of other models and theories would be useful to narrow the choice of viable interpretations.

References

1. T. C. Awes et al., Phys. Rev. C 25, 2361 (1982).
2. E. Holub, et al., Phys. Rev. C 28, 252 (1983).
3. E. Holub, et al., Phys. Rev. C 33, 143 (1986).
4. H. Noll et al., Phys. Rev. Lett. 48, 732 (1982).
5. J. Stachel et al., in Proceedings of the Institute for Nuclear Studies, RIKEN Symposium on Heavy Ion Physics, Tokyo, Japan (1984) unpublished.
6. H. Heckwolf et al., Z. Phys. A 315, 243 (1984).
7. G. R. Young et al., Phys. Rev. C 33, 742 (1986).
8. J. Stevenson et al., Phys. Rev. Lett. 57, 555 (1986).
9. M. Kwato Njock et al., Phys. Lett. B 175, 125 (1986).
10. R. Bertholet et al., Journal de Physique, Colloque C4, supplement au no 8, Tome 47, aout (1986); H. Nifenecker et al., XXIV Int'l. Winter Meeting on Nucl. Phys., Bormio, Italy (1986).
11. N. Alamanos et al., Phys. Lett. B 174, 392 (1986).
12. E. Grosse et al., Europhys. Lett. 2, 9 (1986).
13. E. Grosse, from talk given at the International Workshop on Gross Properties of Nuclei, Hirschegg (1985).

15. D. Vasak, H. Stöcker, B. Müller and W. Greiner, Phys. Lett. 93B, 243 (1980), and D. Vasak, B. Müller and W. Greiner, Physica Scripta 22, 25 (1980); D. Vasak, W. Greiner, B. Müller, T. Stahl and M. Uhlig, Nucl. Phys. A428, 291c (1984); D. Vasak, B. Müller and W. Greiner, J. Phys. G11, 1309 (1985).

16. M. Blann, A. Mignerey and W. Scobel, Nukleonika 21, 335 (1976); M. Blann, Phys. Rev. C 23, 205 (1981); M. Blann, Phys. Rev. C 31, 1245 (1985).

17. M. Blann, Phys. Rev. C 31, 295 (1985).

18 M. Blann, Phys. Rev. C 32, 1231 (1985); Phys. Rev. Lett. 20, 2215 (1985).

19. B. A. Remington, M. Blann and G. F. Bertsch, Phys. Rev. Lett. 57, 2909 (1986); B. A. Remington, M. Blann and G. F. Bertsch, Phys. Rev. C 35, 1720 (1987).

20. G. Bertsch, in "Frontiers in Nuclear Dynamics," ed. by R. A. Broglia and C. H. Dasso (Plenum Press, 1985), p. 277

21. J. Aichelin, Phys. Rev. C 33, 537 (1986)

22. J. J. Molitoris and H. Stöcker, Phys. Rev. C 32, 346 (1985).

23. W. Cassing, T. Biro, U. Mosel, M. Tohyama, and W. Bauer, Phys. Lett. 1818, 217 (1986).

24. W. Bauer, G. F. Bertsch, W. Cassing, U. Mosel, Phys. Rev. C 34, 2127 (1986).

25. G. D. Harp, J. M. Miller and B. J. Berne Phys. Rev. 165, 1166 (1968).

26. G. D. Harp and J. M. Miller, Phys. Rev. C 3, 1847 (1971).

27. B. J. VerWest and R. A. Arndt, Phys. Rev. C 25, 1979 (1982).

28 J. A. Edgington and B. Rose, Nucl. Phys. 89, 523 (1966).

29. M. Blann, Ann. Rev., Nucl. Sci. 25, 123 (1975).

30. J. Bisplinghoff and H. Keuser, Phys. Rev. C 35, 821 (1987).

31. N. Cindro, M. Korolija and E. Holub, "Fundamental Problems in Heavy ion Collisions, " ed. by N. Cindro, et al., p. 301, World Scientific, Singapore (1985).

32. W. Scobel, private communication (1986).

33. G. F. Bertsch, Phys. Rev. C 15, 713 (1977).

14. H. Nifenecker, private communication (1987)

15. D. Vasak, H. Stöcker, B. Müller and W. Greiner, Phys. Lett. 93B, 243 (1980), and D. Vasak, B. Müller and W. Greiner, Physica Scripta 22, 25 (1980); D. Vasak, W. Greiner, B. Müller, T. Stahl and M. Uhlig, Nucl. Phys. A428, 291c (1984); D. Vasak, B. Müller and W. Greiner, J. Phys. G11, 1309 (1985).

16. M. Blann, A. Mignerey and W. Scobel, Nukleonika 21, 335 (1976); M. Blann, Phys. Rev. C 23, 205 (1981); M. Blann, Phys. Rev. C 31, 1245 (1985).

17. M. Blann, Phys. Rev. C 31, 295 (1985).

18 M. Blann, Phys. Rev. C 32, 1231 (1985); Phys. Rev. Lett. 20, 2215 (1985).

19. B. A. Remington, M. Blann and G. F. Bertsch, Phys. Rev. Lett. 57, 2909 (1986); B. A. Remington, M. Blann and G. F. Bertsch, Phys. Rev. C 35, 1720 (1987).

20. G. Bertsch, in "Frontiers in Nuclear Dynamics," ed. by R. A. Broglia and C. H. Dasso (Plenum Press, 1985), p. 277

21. J. Aichelin, Phys. Rev. C 33, 537 (1986)

22. J. J. Molitoris and H. Stöcker, Phys. Rev. C 32, 346 (1985).

23. W. Cassing, T. Biro, U. Mosel, M. Tohyama, and W. Bauer, Phys. Lett. 181B, 217 (1986).

24. W. Bauer, G. F. Bertsch, W. Cassing, U. Mosel, Phys. Rev. C 34, 2127 (1986).

25. G. D. Harp, J. M. Miller and B. J. Berne, Phys. Rev. 165, 1166 (1968).

26. G. D. Harp and J. M. Miller, Phys. Rev. C 3, 1847 (1971).

27. B. J. VerWest and R. A. Arndt, Phys. Rev. C 25, 1979 (1982).

28 J. A. Edgington and B. Rose, Nucl. Phys. 89, 523 (1966).

29. M. Blann, Ann. Rev., Nucl. Sci. 25, 123 (1975).

30. J. Bisplinghoff and H. Keuser, Phys. Rev. C 35, 821 (1987).

31. N. Cindro, M. Korolija and E. Holub, "Fundamental Problems in Heavy Ion Collisions, " ed. by N. Cindro, et al., p. 301, World Scientific, Singapore (1985).

32. W. Scobel, private communication (1986).

33. G. F. Bertsch, Phys. Rev. C 15, 713 (1977).

34. V. R. Brown, Phys. Rev. 177, 1498 (1969); V. R. Brown and J. Franklin, Phys. Rev. C 8, 1706 (1973).

35. J. D. Jackson, Classical Electrodynamics, (Wiley, New York, 1962), p. 703.

36. Che Ming Ko, G. Bertsch and J. Aichelin, Phys. Rev. C 31, 2324 (1985).

37. C. Ciofi degli Atti, E. Pace and G. Salme, Phys. Lett. B 141, 14 (1984).

38. D. Neuhauser and S. E. Koonin, Nucl. Phys. A 462, 163 (1987).

39. D. Morrissey, private communication.

40. M. Blann, Nucl. Phys. A 235, 211 (1974); M. Blann, Proceedings of the International School on Nuclear Physics, Predeal, Romania 1974, ed. A. Ciocanel, p. 249, Bucharest (1976).

Figure Captions

1) Diagrammatic representation of a heavy ion collision in geometric (upper) and energy space. This figure is described in the text.

2) Representation of a Fermi gas nucleus as treated in the Boltzmann master equation. The nucleus is divided into 1 MeV wide energy bins, indexed by i, j, k or l counting from the bottom of the Fermi sea.

3) Calculated and experimentally deduced spectra for the reactions ^{165}Ho(^{12}C,n) at 300 MeV. Experimental points from Refs. 2,3 result from an integration of a moving source fit to experimental yields for the fast component only. Experimental yields for ^{20}Ne projectiles were gated on evaporation residues (ER) as represented by open triangles, and on fission fragments (FF) shown by closed circles. Results for ^{12}C were gated on ER.

Calculated results are shown for the BME with $n = A_p$ in the exciton distribution function, where we assume total excitation is shared by n excitons with equal a-priori probability.

4) Calculated and experimental γ-ray spectra resulting from 140 MeV protons incident on d, C, and Pb targets. Data are from (28). The thin dashed line in the p+d spectrum is the calculation of eq. (7) for X=0. The long dashed curve is the result of folding over the neutron Fermi motion. The solid line is the result of next setting X=1 in eq. (7). The open symbols represents data points. The dot-dash curve is based the results of Ref. (38).

5) Calculated and experimental γ-ray spectra from ^{14}N bombardment of ^{12}C and Pb at 20, 30 and 40 MeV/nucleon. Data are from ref. (8). The solid lines are the predicted spectra based on using eq. (7) with X = 1 in the BME. The dashed curves are the result of using the values from Ref. (38).

6) Results of the BME compared with experimental γ-ray spectra for 30 MeV/μ ^{40}Ar on ^{197}Au. Data are from (9). Calculation uses eq. (7) with X = 1, denoted 'classical X 2'.

7) Calculated (BME) and experimental γ-ray spectra from 44 MeV/μ Kr on C and Ag targets. Experimental results are from ref. (10).

8) Calculatd (BME) and experimental γ-ray spectra from 35 MeV/μ ^{14}N + Ni. Data are from ref. (11).

9) Calculated (solid line) and experimental γ-ray spectra for ^{12}C bombardment of ^{238}U at 84 MeV/μ(top set), and on ^{12}C targets at 84, 74, 60 and 48 MeV/μ, as indicated. Data are from refs. 12 and 13. The dashed line shows the results of a BME

calculation using spectra from ref. (38) as input rather than from eq. (7).

10) Yields of γ-rays above 50 MeV, experimental and calculated, versus beam energy (MeV/nucleon). The ordinate has been scaled for reaction cross section. The solid line is drawn to guide the eye through the experimental data points; the dashed line through the calculated data points. This figure is discussed in the text.

11) Calculated and experimental angular distributions for p + d and p + ^{12}C reactions. Calculations used eq. (7) averaged over internal target nucleon momenta for a single collision process. Data are from ref. (28). The lower calculation has been arbitrarily normalized in absolute magnitude.

12) Experimental and calculated γ-ray angular distributions for 40 MeV/μ ^{14}N on Pb and ^{12}C targets. Data are from ref. (8). The γ-ray energies are shown on the right side of the figure. The dashed line is the result of the first collision only. The solid line uses an estimate of fractional contribution from higher order collisions from the BME to include an estimated isotropic contribution, which has been averaged with the first collision result.

TABLE I. Definition of symbols.

Symbol	Definition
$n_i^X \omega_{i\to i'}^X$	Fraction of population of the nucleons of type X (neutron=n, proton=p) emitted per unit time from a bin at energy i measured from the bottom of the Fermi sea.
$\omega_{ij\to kl}^{XY}$	Rate at which one nucleon of type X at energy i scatters with one nucleon of type Y at energy j into final energies k and l.
g_i^X	Number of states for a particle of type X in a 1 MeV wide energy bin centered at energy i with respect to the Fermi energy.
n_i^X	Fraction of the g_i^X levels in bin i which are occupied at time t.
B_X	Binding energy of a nucleon of type X.
ϵ_i^X	Single particle energy of a nucleon of type X in bin i, measured from the bottom of the Fermi sea.
$\omega_{i\to i'}^X$	Rate at which a particle of type X at energy i with respect to the bottom of the nucleon well and energy i' with respect to the unbound continuum is emitted into the continuum.
$\delta(\epsilon_i^a+\epsilon_j^b-\epsilon_k^c-\epsilon_l^d)$	Unity when initial and final nucleon energies conserve energy, otherwise zero.
E^*	Composite system excitation energy.
V	The nuclear volume, calculated in this work using a square well with radius parameter 1.2×10^{-13} fm.
M	Nucleon mass.
$\sigma^{XY}(\epsilon_i+\epsilon_j)$	Cross section for a free nucleon of type X and energy ϵ_i to collide elastically with a free nucleon of type Y and energy ϵ_j.
$\sigma^{XY\pi^0}(\epsilon_i+\epsilon_j)$	Cross section for a nucleon of type X at energy ϵ_i to collide with a nucleon of type Y at energy ϵ_j to produce a π^0 plus nucleons X and Y with final energies such that mass and energy are conserved.

Table II. Summary of Calculated and Experimental Subthreshold Pion Production Cross-Sections

Projectile Target	MeV Nucleon	Calc. Expt.	Expt. σ_{π^+}(μb)	Emitted[a] Calc. σ_{π^+}(μb)	Ref. Exptl.	Calc. f_{atten}	E*(MeV)
$^{12}C/^{238}U$	84	0.6	174.(21)	110.	b	0.24	936
$^{12}C/^{58}Ni$	84	2.4	72.(9)	175.	b	0.34	835
$^{12}C/^{12}C$	84	0.7	19.(23)	14.	b	0.42	518
$^{12}C/^{238}U$	74	0.7	64.(10)	46.	b	0.24	821
$^{12}C/^{58}Ni$	74	2.4	31.(4)	74.	b	0.34	736
$^{12}C/^{12}C$	74	1.6	8.5(10)	14.	b	0.42	458
$^{12}C/^{238}U$	60	0.7	13.(2)	9.2	b	0.24	661
$^{12}C/^{58}Ni$	60	0.6	19.(23)	11.	b	0.34	597
$^{12}C/^{12}C$	60	0.8	1.7(3)	1.4	b	0.42	374
$^{40}Ar/^{238}U$	44	0.5	6.(3)	2.9	c	0.23	1375
$^{40}Ar/^{119}Sn$	44	0.7	3.7(8)	2.6	c	0.27	1257
$^{40}Ar/^{40}Ca$	44	0.2	2.2(4)	0.33	c	0.33	880
$^{14}N/^{184}W$	35	0.4	0.160(20)	0.058	d	0.26	440
$^{14}N/^{58}Ni$	35	0.5	0.120(15)	0.061	d	0.34	395
$^{14}N/^{27}Al$	35	0.4	0.070(10)	0.028	d	0.38	344
$^{16}O/^{58}Ni$	25	0.04	0.0023	0.001	e	0.30	311
$^{16}O/^{58}Ni$	25	0.3	0.0023	0.0006[f]	e	0.30	311
$^{16}O/^{27}Al$	25	0.08	0.0013	0.0001[f,g]	e	0.37	265

a) Calculated as product of calculated pions/interaction times σ_R times F_{atten}, where $\sigma_R=\{1.2(A_T^{1/3}+A_p^{1/3})\times10^{-13}\}^2\pi$, with A_T and A_p target and projectile mass numbers.

b) H. Noll et al., Phys. Rev. Lett. 48, 732 (1982).
c) H. Heckwolf et al., Z. Phys. A 315, 43 (1984).
d) J. Stachel et al., in Proceedings of the Inst. for Nuclear Studies, RIKEN Symposium on Heavy Ion Physics, Tokyo Japan (1984) unpublished.
e) G. R. Young et al., Phys. Rev. C 33, 742 (1986).
f) Calculated assuming a target Fermi energy of 30 MeV.
g) This experimental excitation is below the threshold for N-N production in a 90° collision. The calculated yield is an artifact of following probability flux rather than individual nucleon populations.

Figure Captions

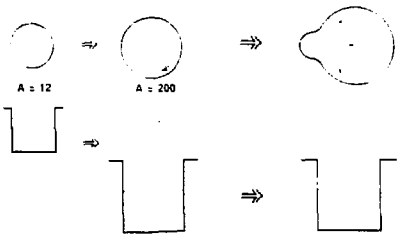

Fig. 1

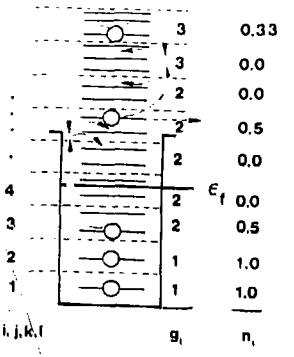

Fig. 2

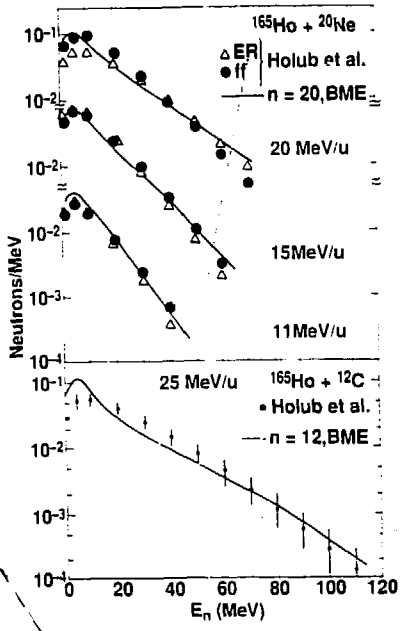

Fig. 3

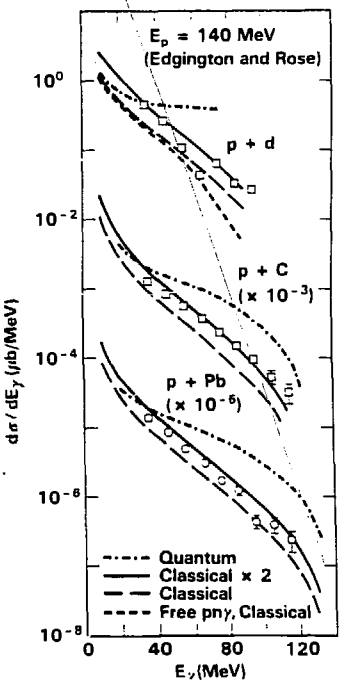

Fig. 4

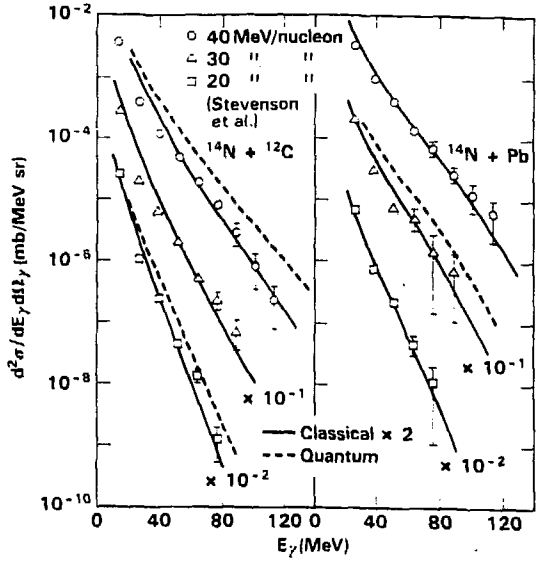

Fig. 5

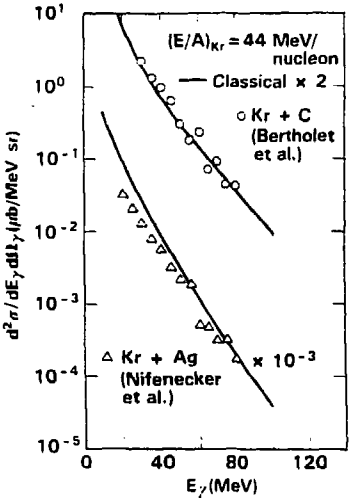

Fig. 7

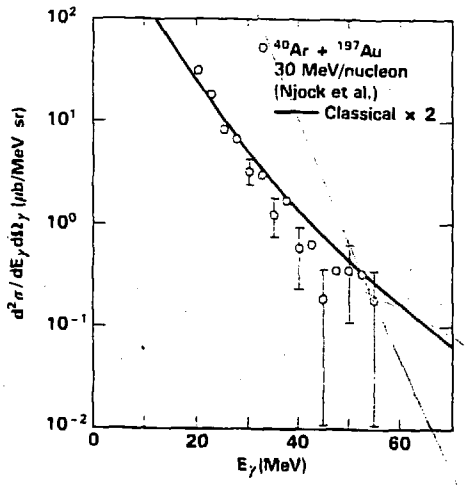

Fig. 6

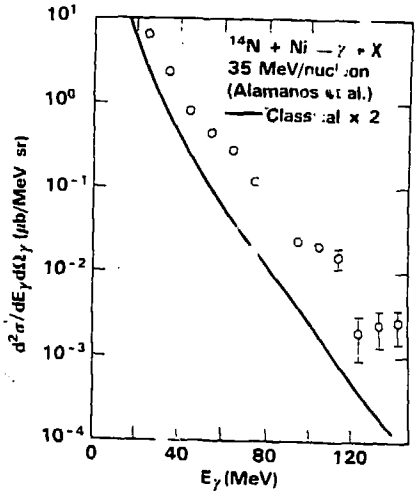

Fig. 8

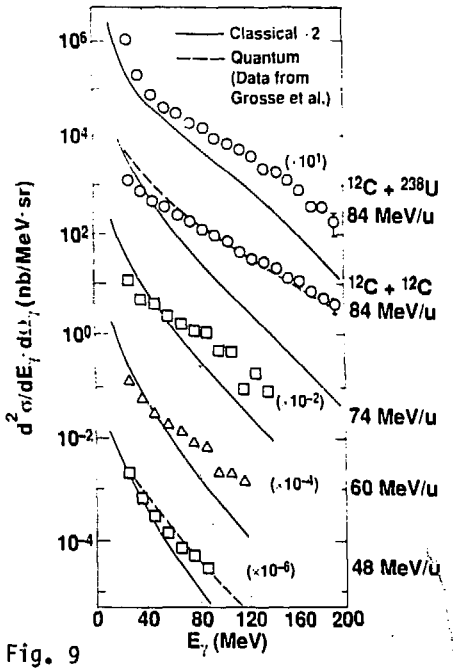

Fig. 9

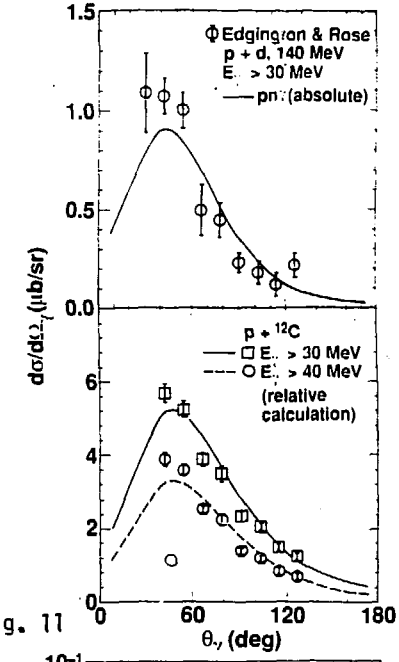

Fig. 11

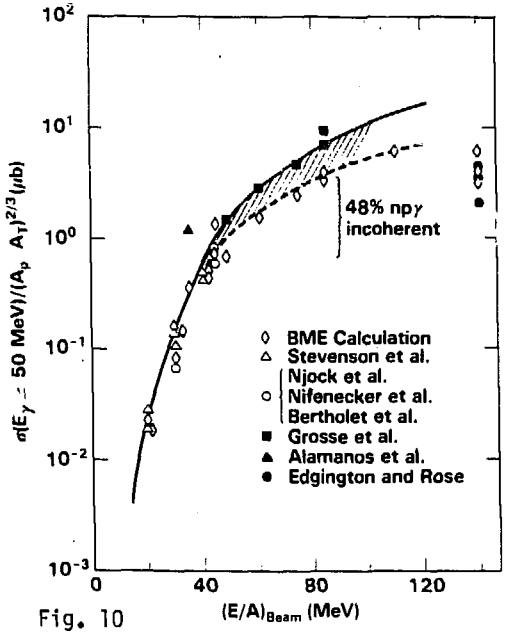

Fig. 10

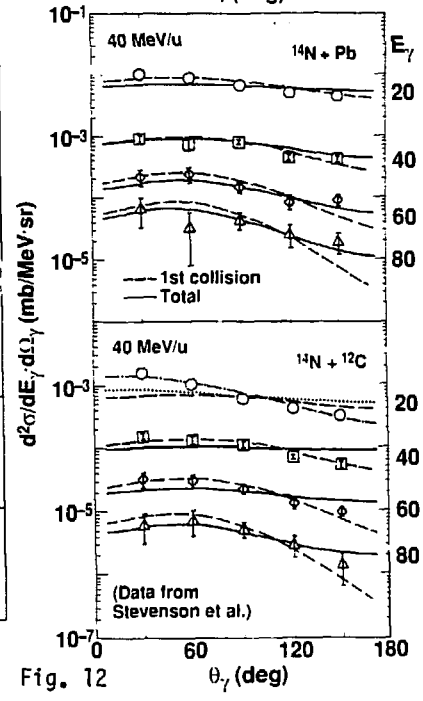

Fig. 12